Int. J. Solids Structures, 1973, Vol. 9, pp. 379 to 394. Pergamon Press. Printed in Great Britain

A QUANTITATIVE STUDY OF A CRYSTALLINE AGGREGATE MODEL

K. S. HAVNER and R. VARADARAJAN†

Department of Civil Engineering, North Carolina State University, Raleigh

Abstract—A discrete aggregate model is applied to the study of theoretical macroscopic response of f.c.c. metal polycrystals. General, dual inequalities of macroscopic plasticity theory are reviewed and exhibited on subsequent yield surfaces in both stress and strain space as calculated for aluminum under biaxial straining. Predicted stress–strain curves are shown corresponding to a partial cycle of loading and reverse loading. The aggregate model contains several thousand crystallographic slip systems, and all quantitative results are obtained through sequential solution of constrained quadratic programming problems governing the incremental crystal shears.

1. INTRODUCTION

IN [1–3] a discrete model for deformation analysis of crystalline aggregates was developed in detail. Aspects of uniqueness and convergence of solution and relationships with theoretical studies by Hill [4, 5] were investigated, and the overall problem (at both small [1, 2] and large [3] strain) was shown to be well-posed within a framework of quadratic programming. In the present paper we present the results of an initial quantitative study of this model under biaxial straining for f.c.c. metal polycrystals, specifically aluminum. We also derive certain explicit equalities connecting microscopic and macroscopic variables that are pertinent to the obtained results and have not previously been given.

2. GENERAL CONSIDERATIONS

At the outset we define a microscopic continuum point-of-view wherein a crystal material "point" has dimensions of order 10^{-3} mm (i.e. $>10^3$ lattice spacings). This is consistent with the minimum level at which a continuum mechanics description of plastic deformation in metals can be judged physically meaningful (see, for example, pertinent discussions in [3] and [6]). The mechanical behavior is taken to be representable via two *kinematically* independent mechanisms of deformation (which are phenomenological averages of complex processes occurring within the lattice volume defined by the "point"). These mechanisms are: (a) elastic (mechanically recoverable) infinitesimal strain of the lattice, and (b) simple glide, on well-defined crystallographic slip systems, which translates material "lines" of points (i.e. glide packets) relative to one another but leaves the (averaged) crystal structure unchanged. Restricting the analysis to small strains, the local constitutive and field equations, in terms of increments, are

$$\delta\boldsymbol{\xi} = \mathscr{D}^T \delta\mathbf{u} = \mathbf{C}\,\delta\boldsymbol{\zeta} + \mathbf{N}^T \delta\boldsymbol{\gamma}, \tag{1}$$

$$\delta\tau_{cr} = \mathbf{H}(\boldsymbol{\gamma})\,\delta\boldsymbol{\gamma}, \tag{2}$$

† Now at: Fairbank Highway Research Station, Federal Highway Administration, Washington, D.C.

and $\mathscr{D}\,\delta\boldsymbol{\zeta} = \mathbf{0}$ (neglecting inertia and body forces). For a critical (i.e. potentially active) slip system:

$$\tau_{cr}^k \equiv \tau_0 + \int \delta\tau_{cr}^k = \mathbf{N}_k\boldsymbol{\zeta}, \tag{3}$$

$$\delta\tau_{cr}^k \geq \mathbf{N}_k\,\delta\boldsymbol{\zeta}, \qquad \delta\gamma_k \geq 0, \tag{4a, b}$$

$$\delta\gamma_k(\delta\tau_{cr}^k - \mathbf{N}_k\,\delta\boldsymbol{\zeta}) = 0 \quad \text{(for each } k\text{)}. \tag{5}$$

In these equations $\boldsymbol{\zeta}$ and $\boldsymbol{\xi}$ are vector representations of micro-stress and strain: $\boldsymbol{\zeta} = (\zeta_{11}, \zeta_{22}, \zeta_{33}, (\sqrt{2})\zeta_{23}, (\sqrt{2})\zeta_{31}, (\sqrt{2})\zeta_{12})$; $\boldsymbol{\xi} = (\xi_{11}, \xi_{22}, \xi_{33}, (\sqrt{2})\xi_{23}, (\sqrt{2})\xi_{31}, (\sqrt{2})\xi_{12})$. The operator $\mathscr{D}$ is a three by six matrix representation of the spatial gradient, $\mathbf{u}$ is the displacement, $\mathbf{C}$ is the positive-definite crystal elastic compliance matrix referred to the specimen axes, and $\mathbf{N}$ is the N by six transformation matrix between these axes and the local crystallographic slip systems, $\mathbf{N}_k$ denoting the kth row vector (see Appendix). The $\delta\boldsymbol{\gamma}$ are incremental plastic shears, τ_{cr}^k is a critical shear stress (crystal shear strength) initially equal to τ_0, and $\mathbf{H}(\boldsymbol{\gamma})$ is a general crystal hardening matrix [4, 7]. Opposite senses of slip in the same crystallographic slip system are denoted by distinct k's so that $\delta\gamma_k$ is always non-negative. (Throughout the paper, juxtaposition of matrix and vector or vector and vector implies inner product multiplication.)

Consider a thin-walled metal tube subjected to, say, axial load and internal pressure. The wall thickness of specimens studied experimentally in combined loading tests is often in the range 1–2 mm, with from 10–30 grains through the thickness (see [8, 9], for example). Thus, as an idealization of the physical situation, we assume a thickness of 1 mm and define a unit cube $V = 1\ \text{mm}^3$ containing on the order 1000 crystal grains in the corresponding "flat sheet" representation (i.e. a *macroscopic* plane stress problem). Further, we wish the mathematical model to correspond to a macroscopically homogeneous physical specimen (that is, one for which strain gage readings, over distances of at least 1 mm on the surface, are essentially uniform from one location to another). We therefore require all the unit cubes to deform identically and take the longitudinal and transverse faces to be planes of symmetry under biaxial macroscopic straining. (For additional discussion see [1].) Thus, for quasi-static deformation, we adopt as a model for analysis a unit cube (of generally anisotropic crystals) on each of whose faces either (1) a particular incremental displacement component is prescribed, to give the appropriate *macroscopic* strain increment, or (2) the associated traction is zero.

3. ANALYTICAL AVERAGING

As shown in [1], the model of identically deforming cubes satisfies exactly the following averaging theorem for statically admissible stress fields and kinematically admissible strain fields (with a bar above a vector or scalar field denoting the aggregate volume average),

$$\overline{\boldsymbol{\zeta}\boldsymbol{\xi}} = \bar{\boldsymbol{\zeta}}\bar{\boldsymbol{\xi}}, \tag{6}$$

and appropriate definitions of macroscopic stress and strain are

$$\boldsymbol{\sigma} = \bar{\boldsymbol{\zeta}}, \qquad \boldsymbol{\varepsilon} = \bar{\boldsymbol{\xi}}. \tag{7a, b}$$

(These relationships were derived first by Bishop and Hill [10], based upon a "non-correlation" hypothesis, and restated by Kocks [11]. They also are satisfied by boundary conditions on a macro-element of either uniform loading or uniform constraint, as shown by Hill [5, 12], and for purposes of theoretical studies (6) may be considered a minimum prescription of macroscopically uniform fields. For further discussion of the essentially equal viability of the various postulates of identical deformation, uniform loading, or uniform constraint see [13].)

Let $\delta\boldsymbol{\xi}^{(e)}$ denote the incremental micro-strain field determined by assuming (hypothetical) elastic response of the aggregate to an imposed macrostrain increment $\delta\boldsymbol{\varepsilon}$:

$$\delta\boldsymbol{\xi}^{(e)} = \mathscr{D}^T \delta\mathbf{u}^{(e)} = \boldsymbol{\Upsilon}\, \delta\boldsymbol{\varepsilon} \tag{8}$$

in which $\boldsymbol{\Upsilon}$ is a tensor (matrix) function of position within V due to the elastic heterogeneity of the cube. From (6) and (8), a symmetric, inverse elastic compliance matrix of the aggregate can be defined as [1]

$$\mathbf{C}_M^{-1} = \overline{\boldsymbol{\Upsilon}^T \mathbf{C}^{-1} \boldsymbol{\Upsilon}}. \tag{9}$$

Furthermore, let $\mathbf{C}\boldsymbol{\zeta}^{(e)}$ denote that portion of the microstrain field that would be recovered if the specimen could be *elastically* unloaded to zero macrostress, so that [1]

$$\delta\boldsymbol{\zeta}^{(e)} = \mathbf{C}^{-1} \boldsymbol{\Upsilon} \mathbf{C}_M\, \delta\boldsymbol{\sigma}. \tag{10}$$

Then, (apparent) incremental macroscopic plastic strain is determined as [(6), (9), (10)]

$$\delta\boldsymbol{\varepsilon}^p = \overline{\delta\boldsymbol{\xi} - \mathbf{C}\, \delta\boldsymbol{\zeta}^{(e)}} = \delta\boldsymbol{\varepsilon} - \mathbf{C}_M\, \delta\boldsymbol{\sigma}. \tag{11}$$

Denoting $\boldsymbol{\zeta}^r = \boldsymbol{\zeta} - \boldsymbol{\zeta}^{(e)}$ (the residual microstress field that would remain upon elastic unloading to $\boldsymbol{\sigma} = \mathbf{0}$) we find from (6), (7) and (10), corresponding to any $\delta\boldsymbol{\sigma}$ producing slip,

$$\delta\boldsymbol{\sigma} \mathbf{C}_M\, \delta\boldsymbol{\sigma} = \overline{\delta\boldsymbol{\zeta}^{(e)} \mathbf{C}\, \delta\boldsymbol{\zeta}^{(e)}} = \overline{\delta\boldsymbol{\zeta} \mathbf{C}\, \delta\boldsymbol{\zeta}} - \overline{\delta\boldsymbol{\zeta}^r \mathbf{C}\, \delta\boldsymbol{\zeta}^r}. \tag{12}$$

Also, from (1), (4a) and (5),

$$\delta\boldsymbol{\sigma}\, \delta\boldsymbol{\varepsilon} = \overline{\delta\boldsymbol{\zeta} \mathbf{C}\, \delta\boldsymbol{\zeta}} + \overline{\delta\tau_{cr}\, \delta\gamma}. \tag{13}$$

Thus, upon substituting (11) and (12),

$$\delta\boldsymbol{\sigma}\, \delta\boldsymbol{\varepsilon}^p = \overline{\delta\tau_{cr}\, \delta\gamma} + \overline{\delta\boldsymbol{\zeta}^r \mathbf{C}\, \delta\boldsymbol{\zeta}^r}, \tag{14}$$

and for $\mathbf{H}(\boldsymbol{\gamma})$ at least positive-semidefinite $\delta\boldsymbol{\sigma}\, \delta\boldsymbol{\varepsilon}^p > 0$, which result was proved by Hill [5] (although he did not develop an explicit equation for $\delta\boldsymbol{\sigma}\, \delta\boldsymbol{\varepsilon}^p$ in terms of micro-fields, as here). The inequality was apparently first set-down as a fundamental postulate of macroscopic plasticity theory by Prager [14] and was subsequently argued on the basis of a concept of material stability by Drucker [15, 16].

We now develop a set of relationships dual to the above. Let $\boldsymbol{\zeta}^s = \boldsymbol{\zeta} - \mathbf{C}^{-1}\boldsymbol{\xi}^{(e)}$ denote the microstress field due to internal slip and self-straining [1] and define incremental macroscopic "plastic stress" (or "negative slip stress") as

$$\delta\boldsymbol{\sigma}^p = -\overline{\delta\boldsymbol{\zeta}^s} = \mathbf{C}_M^{-1}\, \delta\boldsymbol{\varepsilon} - \delta\boldsymbol{\sigma}. \tag{15}$$

Then, from (6), (7) and (8), for any $\delta\varepsilon$ producing slip,

$$\delta\varepsilon \mathbf{C}_M^{-1}\,\delta\varepsilon = \overline{\delta\xi^{(e)}\mathbf{C}^{-1}\,\delta\xi^{(e)}}$$
$$= \overline{\delta\zeta\mathbf{C}\,\delta\zeta} + \overline{\delta\zeta^s\mathbf{C}\,\delta\zeta^s} + 2\,\overline{\delta\tau_{cr}\,\delta\gamma}. \tag{16}$$

Thus, substituting from (13) and (15),

$$\delta\varepsilon\,\delta\sigma^p = \overline{\delta\tau_{cr}\,\delta\gamma} + \overline{\delta\zeta^s\mathbf{C}\,\delta\zeta^s}, \tag{17}$$

and we obtain the inequality $\delta\varepsilon\,\delta\sigma^p > 0$. This result does not appear to have been given previously, although it is pertinent to the "stress theory" of plasticity proposed by Trifan [17].†

We state without proof the dual orthogonality (or "generalized normality") conditions $\delta\sigma^*\,\delta\varepsilon^p \leq 0$ and $\delta\varepsilon^*\,\delta\sigma^p \leq 0$, which follow immediately from an inequality established by Hill [5]. ($\delta\sigma^*$, $\delta\varepsilon^*$ are any associated macroscopic pair corresponding to purely elastic response of the aggregate.) Summarizing, the crystalline aggregate model satisfies the fundamental macroscopic inequalities

$$\delta\sigma\,\delta\varepsilon^p > 0, \qquad \delta\sigma^*\,\delta\varepsilon^p \leq 0 \tag{18a, b}$$

and their dual pair

$$\delta\varepsilon\,\delta\sigma^p > 0, \qquad \delta\varepsilon^*\,\delta\sigma^p \leq 0. \tag{19a, b}$$

These results will be exemplified on the calculated subsequent yield surfaces displayed in Section 6.

In closing this discussion it is worth noting the relationship between (apparent) macroscopic plastic strain and the volume average of micro-plastic strain $\delta\xi^p \equiv \mathbf{N}^T\,\delta\gamma$. We find

$$\delta\varepsilon^p = \overline{\delta\xi^p} + \overline{\mathbf{C}\,\delta\zeta^r}, \tag{20}$$

which follows from (1) and (11). For an aggregate of hypothetical isotropic crystals $\mathbf{C} = \mathbf{C}_M$ and the last term is zero from (7a) (since ζ^r is statically admissible under zero macrostress), whence $\delta\varepsilon^p$ reduces to the straightforward volume average $\overline{\delta\xi^p}$. This is the definition of macroscopic plastic strain adopted by Lin in an important series of papers (for a complete bibliography, see his recent review article [18]) and also shown to be an appropriate choice for this special case by Rice [19]. For an aggregate of orthotropic crystals we return to the general expression (20) or its equivalent (11).

4. THE QUANTITATIVE MODEL

Introducing the approximation of kinematically admissible, piecewise linear displacement functions, we obtain a discretized model of the heterogeneous aggregate continuum whose formal solution reduces to the following quadratic programming problem [1]. Minimize the convex functional

$$I(\delta\Gamma) = \tfrac{1}{2}\,\delta\Gamma\mathbf{P}\,\delta\Gamma - \delta\Gamma\bar{\mathbf{N}}\mathbf{Q}\mathbf{B}_0\,\delta\mathbf{U}^0 \tag{21}$$

† Since submitting the manuscript, the authors' attention has been called to a paper by R. Hill, *Prik. Mat. Mekh.* **35**, 31 (1971), wherein the dual inequality and equations equivalent to (14) and (17) are derived.

subject to $\delta\boldsymbol{\Gamma} \geq \mathbf{0}$, where $\mathbf{P} = \overline{\mathbf{H}} + \overline{\mathbf{N}}\mathbf{Q}\overline{\mathbf{N}}^T$ is positive-definite over critical systems. Alternatively, we have the dual problem [3]: maximize $-\delta\boldsymbol{\Gamma}\mathbf{P}\,\delta\boldsymbol{\Gamma}$ subject to

$$\mathbf{P}\,\delta\boldsymbol{\Gamma} - \overline{\mathbf{N}}\mathbf{Q}\mathbf{B}_0\,\delta\mathbf{U}^0 \geq \mathbf{0}. \tag{22}$$

In the above, $\delta\mathbf{U}^0$ is the vector of prescribed surface displacements corresponding to incremental macroscopic strain $\delta\boldsymbol{\varepsilon}$, $\delta\boldsymbol{\Gamma} = (\ldots, \delta\gamma_{(q)}, \ldots)$ with q denoting a tetrahedral crystallite element of volume V_q, $\overline{\mathbf{H}} = \lceil \mathbf{H}_{(q)} V_q \rfloor$ (i.e. diagonal in sub-matrices), $\overline{\mathbf{N}} = \lceil \mathbf{N}_c \rfloor$ (referred to the crystal lattice axes), and

$$\mathbf{Q} = \mathbf{S}[\mathbf{I} - \mathbf{B}_i\mathbf{K}^{-1}\mathbf{B}_i^T\mathbf{S}] \tag{23}$$

wherein $\mathbf{I}$ is an identity matrix, $\mathbf{S} = \lceil \mathbf{C}_c^{-1} V_q \rfloor$ (again referred to the crystal axes), and $\mathbf{K} = \mathbf{B}_i^T\mathbf{S}\mathbf{B}_i$ (the symmetric, positive-definite elastic "stiffness" matrix of the aggregate). The matrices $\mathbf{B}_i$ and $\mathbf{B}_0$ (defined over nodes J of unknown and prescribed displacements, respectively) are composed of six by three elements $\mathbf{B}_{qJ} = \mathbf{A}_{(q)}\mathscr{D}^T\phi_q^J(\mathbf{x})$ ($\mathbf{0}$ if J is not a node of q). $\mathbf{A}_{(q)}$ is the stress vector transformation matrix from the cube axes x_i to the crystal axes (determined by the grain orientation), and for any J of q

$$\phi_q^J(\mathbf{x}) = \alpha_q^J + \beta_q^{Ji} x_i. \tag{24}$$

The repeated suffix indicates summation and the constants α_q^J, β_q^{Ji} are determined from the nodal coordinates of q through the equations $\phi_q^J(\mathbf{x}^M) = \delta^{JM}$, $J, M = 1, \ldots, 4$, with δ^{JM} the Kronecker delta. The model is a rational approximation within polycrystalline plasticity theory in that discretized stress and strain increment fields strictly converge to the corresponding micro-continuum fields as element sizes are reduced within crystal grains [2].

Successive quantitative solutions of (21) and evaluations of the macro-variables have been accomplished, followed a prescribed strain path, for an aggregate of f.c.c. aluminum crystals. Because of extensive computer time and storage requirements the model calculated was limited to approximately 400 grains within the unit cube, one quadrant of which is represented in Fig. 1. Each sub-cube contains six equal-volume tetrahedral crystallites, with a typical one as shown in the figure. The orientations of the crystal lattice axes ξ_J ($\langle 100 \rangle$ in Miller index notation) are defined by the Euler angles ϕ, θ, ψ (see Appendix),

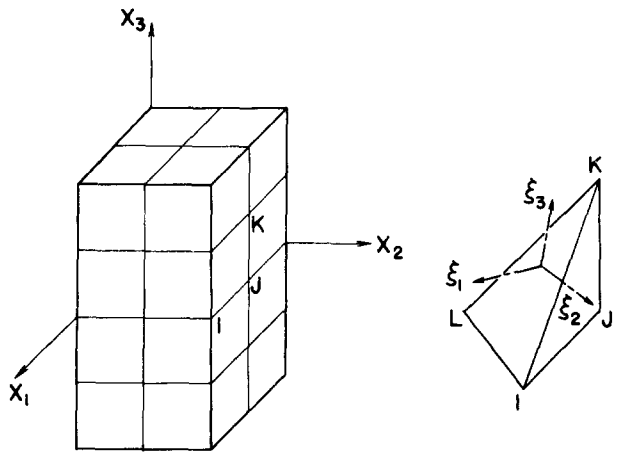

FIG. 1. One quadrant of unit cube and a typical tetrahedral crystallite.

these having been chosen for the various grains so as to simulate a statistically isotropic specimen. Each crystallite has twelve crystallographically equivalent slip systems $\{111\}\langle 1\bar{1}0\rangle$, or twenty-four counting opposite senses of slip as distinct systems, giving a total of 2304 within the quadrant. The faces $x_3 = \pm 1/2$ are free and macroscopic biaxial strains $\varepsilon_{11}, \varepsilon_{22}$ are imposed by specifying uniform normal displacements on the faces $x_1, x_2 = 1/2$. (We take $x_1, x_2 = 0$ to be planes of symmetry, hence normal displacements are zero on these faces.) The influence function Υ (equation 8), piecewise constant in the discrete model, is evaluated from separate elastic solutions for the states $\varepsilon_{11} = 1$, $\varepsilon_{22} = 0$ and $\varepsilon_{22} = 1$, $\varepsilon_{11} = 0$. The general elastic solution for the strains $\delta\xi_{(q)}^{(e)}$ is [1, 2]

$$\delta\mathbf{E}^{(e)} \equiv (\ldots, \delta\xi_{(q)}^{(e)}, \ldots) = \bar{\mathbf{A}}^T\mathbf{S}^{-1}\mathbf{Q}\mathbf{B}_0\,\delta\mathbf{U}^0 \tag{25}$$

in which $\bar{\mathbf{A}} = \lceil \mathbf{A}_{(q)} \rfloor$. (For an exterior node J at which only one or two displacement components are unknown, the super-column of $\mathbf{B}_{qJ}$ in (23) and (25) is divided between $\mathbf{B}_i$ and $\mathbf{B}_0$.) The classical Taylor hardening rule [20, 21] was adopted for the calculation of crystal shears, whence $\mathbf{H} = h\mathbf{1}$. ($\mathbf{1}$ is an N by N matrix all of whose elements are unity, and h is a hardening modulus to be discussed in Section 5.)

5. THE COMPUTATIONAL PROBLEM

For the numerical elastic analysis, which is almost trivial, a much finer representation of the crystalline aggregate could have been selected. The restriction for computational purposes to the moderately coarse model of Fig. 1 was dictated by considerations of the magnitude of the plastic analysis, since even with this model one must keep track of a large number of slip systems throughout the deformation history. To assess the adequacy of the model's elastic behavior, we compare computed with expected results as follows. Since the boundary value problem of the unit cube corresponds to a macroscopic plane stress state σ_{11}, σ_{22}, only a reduced elastic compliance $\mathbf{C}_M$ can be determined from (9). For a statistically isotropic specimen with a very large number of grains we would have $(C_M)_{11} = (C_M)_{22} = 1/E$ and $(C_M)_{12} = (C_M)_{21} = -\nu/E$. The values computed for the quantitative model from (8), (9) and (25), in units of $10^{-3}\,\text{mm}^2/\text{kg}$, are $(C_M)_{11} = 0{\cdot}1420$, $(C_M)_{22} = 0{\cdot}1388$, $(C_M)_{12} = (C_M)_{21} = -0{\cdot}04985$. The first two values differ by less than two and one-half per cent. Taking their average (0·1404) and converting to psi we obtain $E = 10{\cdot}15 \times 10^6$ psi, $\nu = 0{\cdot}354$ and $G = 3{\cdot}74 \times 10^6$ psi. These results probably could be improved upon without further refining the model because the choice of orientations (fully described for all grains in [22]) was unnecessarily weighted in favor of the angle ψ, and a more balanced distribution relative to the axes x_1, x_2 could have been selected. Be that as it may, the results were judged acceptable and representative of a nearly isotropic aggregate specimen.

In developing a computer code for determination of the incremental plastic shears via (21), several standard quadratic programming routines were considered and compared [22]. The one adopted is a procedure due to Hildreth and D'Esopo, described in [23], for which it was found convenient to have the full matrix $\bar{\mathbf{N}}\mathbf{Q}\bar{\mathbf{N}}^T$ available in fast access auxiliary storage. The matrix was maintained at minimum size by redefining both senses of slip as a single system. The necessary sign modifications follow. Let $\mathbf{P}_+^s = \bar{\mathbf{N}}_+\mathbf{Q}\bar{\mathbf{N}}_+^T$ denote the reduced (1152 by 1152) matrix for one quadrant of the cube, wherein $\bar{\mathbf{N}}_+$ corresponds to the arbitrarily chosen positive senses of slip. Also denote $\mathbf{F}_+ = \mathbf{N}_+\mathbf{Q}\mathbf{B}_0\mathbf{U}^0$. Consider two

critical systems j, k within the aggregate and denote the associated elements of $\mathbf{P}^s_+$ by $p_{jj}, p_{jk} = p_{kj}, p_{kk}$ and of $\mathbf{F}_+$ by f_j, f_k. Then, if k is critical in the positive sense ($f_k > 0$) whereas j is critical in the negative sense ($f_j < 0$), we can still pose the quadratic programming problem (21) [or (22)] with both $\delta\gamma_j$ and $\delta\gamma_k$ constrained to be non-negative simply by changing the signs of $p_{jk} = p_{kj}$ and δf_j. (If both systems are critical in the negative sense, we change only the signs of δf_j and δf_k.) After the calculations for the shears have been completed, the signs are changed back (including the sign of $\delta\gamma_j$, which now will be negative) before calculating the incremental stresses $\delta\zeta_{s(q)}$ given by [1, 2]

$$\delta\boldsymbol{\Sigma} \equiv (\ldots, \delta\zeta_{s(q)} V_q, \ldots) = \bar{\mathbf{A}}^T \mathbf{Q}(\mathbf{B}_0\, \delta\mathbf{U}^0 - \bar{\mathbf{N}}^T\, \delta\boldsymbol{\Gamma}). \tag{26}$$

The final step in defining the computational model is the selection of the work-hardening modulus h, traditionally the slope of the resolved shear stress–strain curve $\tau(\gamma)$ from a tensile (or compressive) test of a single crystal. A representative (but certainly not definitive) value of 7·5 kg/mm^2 was chosen, influenced by the general discussions regarding experimental curves for variously oriented single crystals of aluminum in [11] and [24] and taking into account the restriction of this study to the early stages of plastic deformation in crystalline aggregates. (The value of initial critical stress τ_0 is immaterial if we adopt a consistent, dimensionless presentation of the numerical results, as explained in the next section.)

6. NUMERICAL RESULTS AND DISCUSSION

It is evident from (21)–(23), (25) and (26) that the solution to the discrete model can be expressed in terms of new deformation variables $\delta\mathbf{U}^0/(2\tau_0/\mu)$, $\delta\boldsymbol{\gamma}/(2\tau_0/\mu)$, $\delta\boldsymbol{\xi}/(2\tau_0/\mu)$ and dimensionless stresses $\delta\boldsymbol{\zeta}/(2\tau_0)$, wherein μ is a representative crystal or aggregate elastic modulus. Moreover, for Taylor hardening [from (2) and (3)]

$$\left(\frac{\tau_{cr}}{2\tau_0}\right)_{(q)} = \frac{1}{2} + \sum_k \frac{h}{\mu}\left(\frac{\gamma_k}{2\tau_0/\mu}\right)_{(q)}. \tag{27}$$

Thus we conclude that, for a given choice of grain distributions within the aggegate, results presented in terms of dimensionless variables $\boldsymbol{\sigma}/(2\tau_0)$ and $\boldsymbol{\varepsilon}/(2\tau_0/\mu)$ are independent of τ_0 and depend only upon the parameter h/μ. Adoption of these variables herein will enable us to circumvent the very difficult problem of predicting quantitative levels of macroscopic yielding comparable to the customary stresses experienced even in soft, commercially pure aluminum. (Compare, for example, the numerical results in [18].) In large measure this difficulty can be attributed to what metallurgists call "grain size effects." (See [25] for a critical review.) Hutchinson also has chosen to present all results in dimensionless form in [26], although he variously selects both E and G for μ.

The prescribed macrostrain path for the present study of the quantitative aggregate model is given by Fig. 2, with the macroscopic stress path predicted from the calculations shown in Fig. 3. The corresponding stress–strain curves are presented in Figs. 4 and 5. The complete strain path represents more than 500 incremental steps. At point C, just prior to strain reversal and elastic unloading, 177 slip systems were simultaneously active within the ninety-six crystallites of the quadrant (Fig. 1). At point E, prior to termination of the straining sequence, 239 slip systems were active. At point B, corresponding to an abrupt change in the macrostrain and macrostress paths, the number of active systems dropped

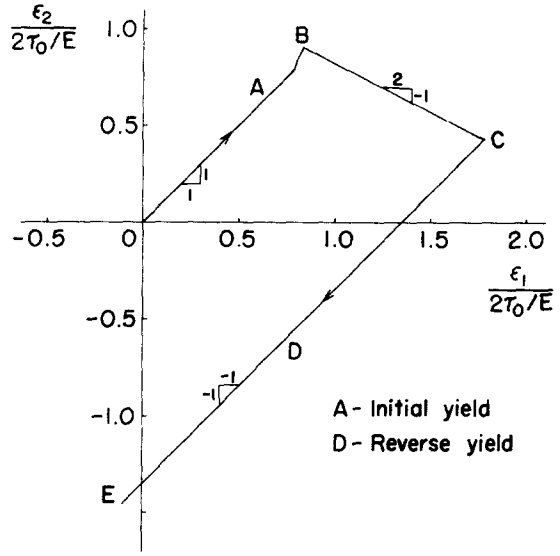

FIG. 2. Prescribed strain path.

from 149 to 104 although the same number of systems were critical just before and during the incremental step.

After solution of the programming problem (21) for a given macrostrain increment, the new values of resolved shear stresses in all crystallographic slip systems throughout the

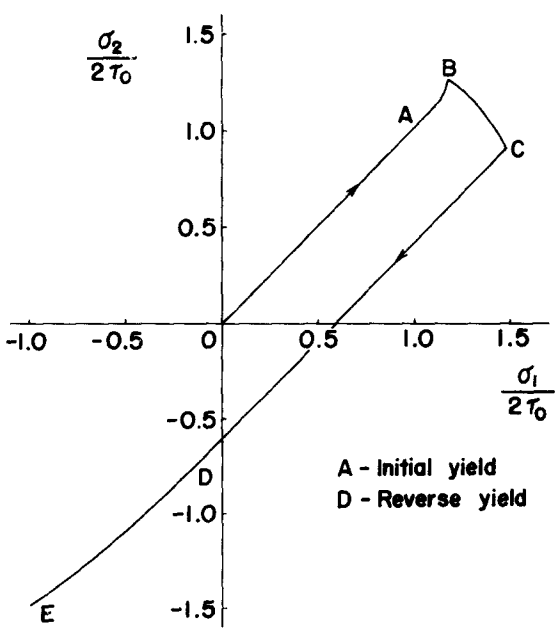

FIG. 3. Predicted stress path.

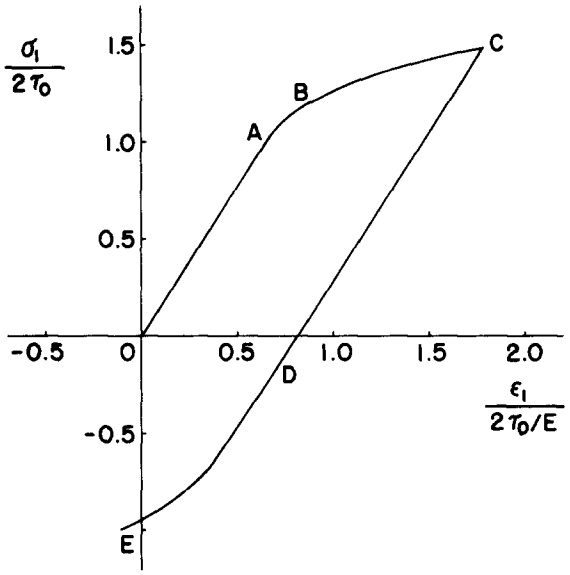

FIG. 4. Stress-strain curve in x_1 direction.

aggregate must be determined. Since the $\xi^{(e)}_{\gamma(q)}$ are known from (25), it is convenient to compute only changes in $\tau^s = \mathbf{N}\zeta^s$. From (25), (26), and the definition of ζ^s, Section 3, we find

$$\delta\mathbf{T}^s \equiv (\ldots, \delta\tau^s_{(q)} V_q, \ldots) = \bar{\mathbf{N}}\mathbf{Q}\bar{\mathbf{N}}^T \delta\boldsymbol{\Gamma}. \tag{28}$$

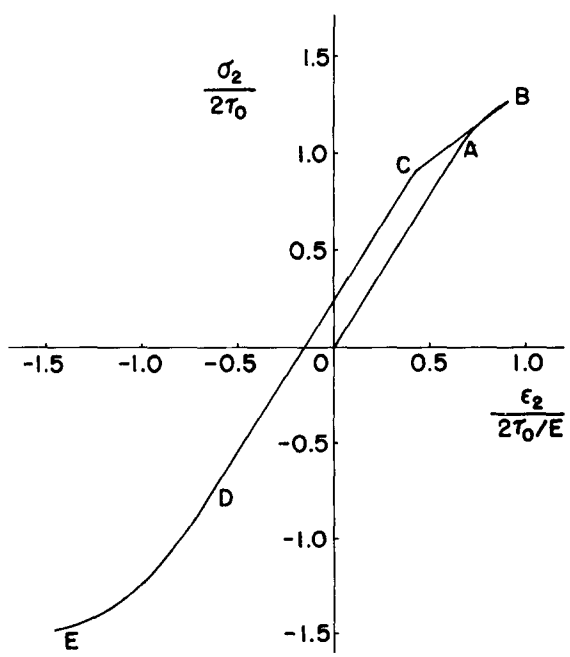

FIG. 5. Stress-strain curve in x_2 direction.

Upon calculation of the new values for τ_{cr} and $\boldsymbol{\tau}^s$, we locate the kth yield hyperplane in macrostrain space by the equation [1]

$$D_k^{\varepsilon} = (\tau_{cr} - \tau_k^s)/\|\mathbf{N}_k\mathbf{C}^{-1}\boldsymbol{\Upsilon}\|_{(q)} \tag{29}$$

which gives the distance to the plane whose normal direction is defined by the vector $(\mathbf{N}_k\mathbf{C}^{-1}\boldsymbol{\Upsilon})_{(q)}$. Similarly, from the definition of $\boldsymbol{\zeta}^r$ (Section 3),

$$\tau_k^r = \tau_k^s + (\mathbf{N}_k\mathbf{C}^{-1}\boldsymbol{\Upsilon})_{(q)}(\boldsymbol{\varepsilon} - \mathbf{C}_M\boldsymbol{\sigma}), \tag{30}$$

and the distance to the kth yield hyperplane plotted in macrostress space is [1]

$$D_k^{\sigma} = (\tau_{cr} - \tau_k^r)/\|\mathbf{N}_k\mathbf{C}^{-1}\boldsymbol{\Upsilon}\mathbf{C}_M\|_{(q)} \tag{31}$$

with normal direction $(\mathbf{N}_k\mathbf{C}^{-1}\boldsymbol{\Upsilon})_{(q)}\mathbf{C}_M$. A computer code was written to plot these various planes in the respective macrostress $(\sigma_{11}, \sigma_{22})$ and macrostrain $(\varepsilon_{11}, \varepsilon_{22})$ spaces at selected stages of the deformation, the inner bounds constituting the macroscopic yield surfaces. Since the aggregate model is nearly elastically isotropic, the initial yield surface in stress space is very close to the Tresca criterion. (It is exactly the Tresca surface for aggregates containing a large number of isotropic crystals.) Subsequent yield surfaces are presented in Figs. 6–8 (stress space) and Figs. 9–11 (strain space) corresponding to points B, C, and E of the strain path, Fig. 2. In each figure a representative "fan" defining the range of critical slip systems at the current stress or strain point is shown and the appropriate incremental vector pair $\delta\boldsymbol{\sigma}, \delta\boldsymbol{\varepsilon}^p$ or $\delta\boldsymbol{\varepsilon}, \delta\boldsymbol{\sigma}^p$ is displayed. We can see the geometric confirmation of the macroscopic inequalities (18a, b) on the constructed yield surfaces in stress space, with the inequalities (19a, b) confirmed on the yield surfaces in strain space. Lastly, in Figs. 12 and 13 the yield surfaces at C and E of Fig. 2 are shown superimposed upon the respective initial yield surfaces. (Several intermediate yield surfaces are given in [22] together with a detailed description of all computer codes.)

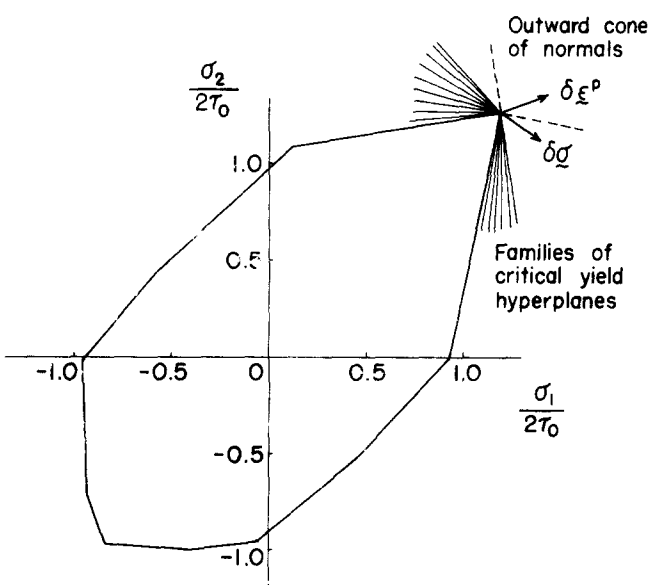

FIG. 6. Subsequent yield surface in stress space at B, showing incremental stress and plastic strain vectors.

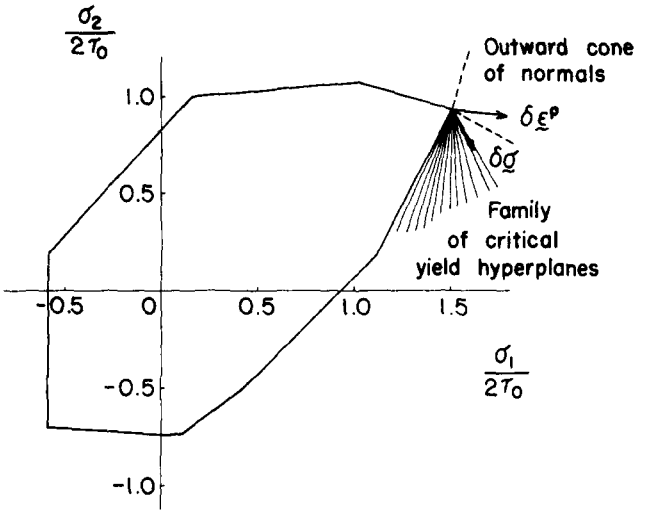

FIG. 7. Subsequent yield surface in stress space at C, showing incremental stress and plastic strain vectors.

In the interpretation and assessment of the above results, several points should be borne in mind. First, we are investigating only a *model* of aggregate behavior (and a discretized one at that!) based upon a relatively simple though physically descriptive theory. However, the model is "self-consistent" and the discretization is demonstrably convergent

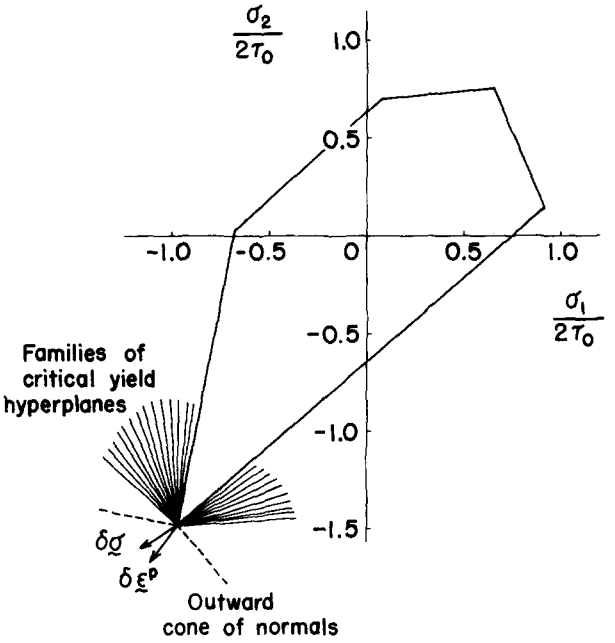

FIG. 8. Subsequent yield surface in stress space at E, showing incremental stress and plastic strain vectors.

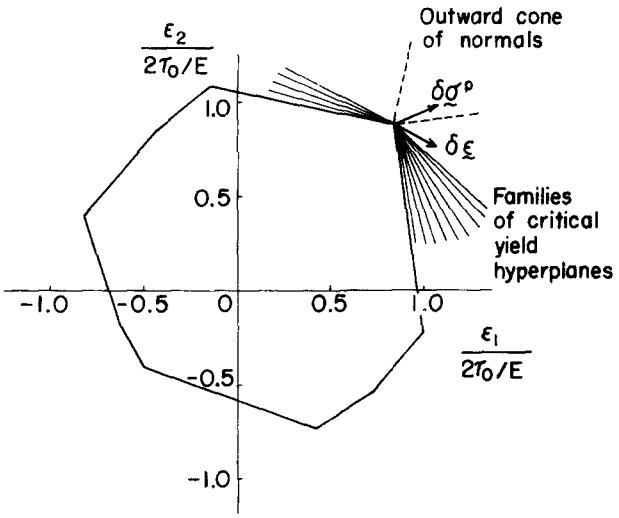

FIG. 9. Subsequent yield surface in strain space at B, showing incremental strain and plastic stress vectors.

[2]. Consequently, the model is at the least an appropriate *type* of idealization for quantitative study. Secondly, the kind of "yield surface" (as limit of purely elastic response) defined herein can never be measured experimentally, even if the quantitative model could match a representative specimen volume-element grain by grain. The most precisely defined yield surfaces attainable through experiment require additional plastic strain increments of at least several microinches/inch (see [27], for example). At most, these constructed surfaces are sharply rounded in the vicinity of a stress point, but they do not exhibit the pointed

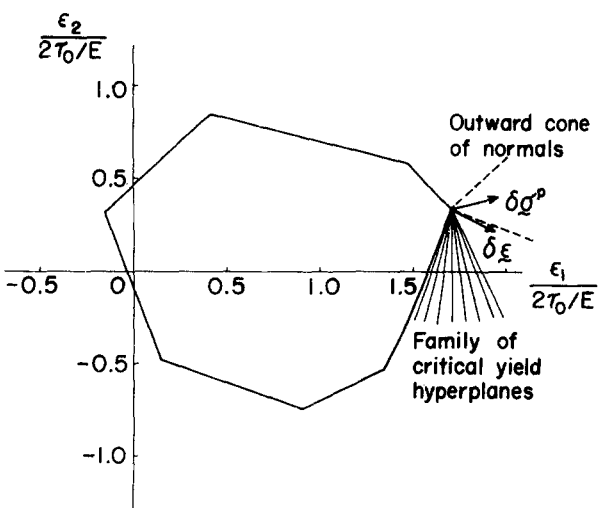

FIG. 10. Subsequent yield surface in strain space at C, showing incremental strain and plastic stress vectors.

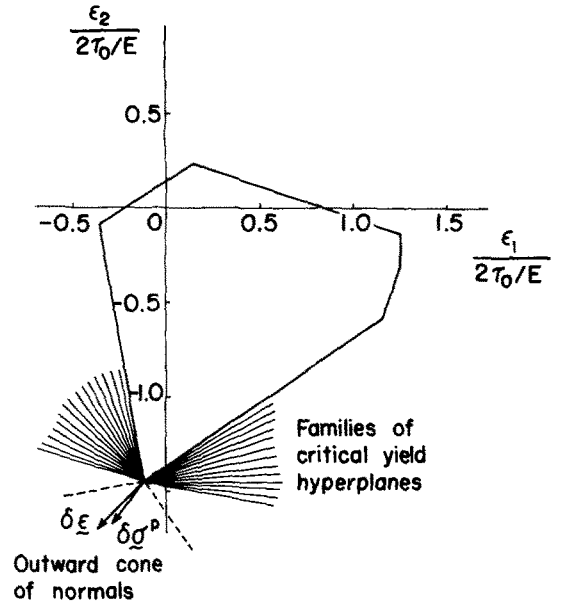

FIG. 11. Subsequent yield surface in strain space at E, showing incremental strain and plastic stress vectors.

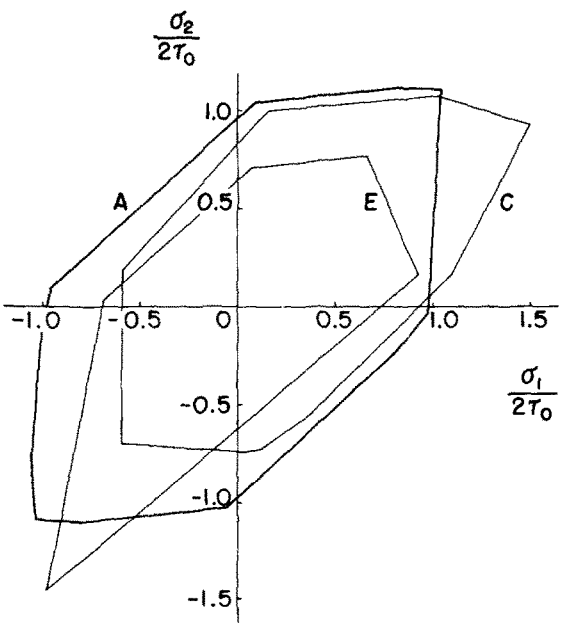

FIG. 12. Superposition of initial yield surface (A) in stress space with subsequent yield surfaces at C and E.

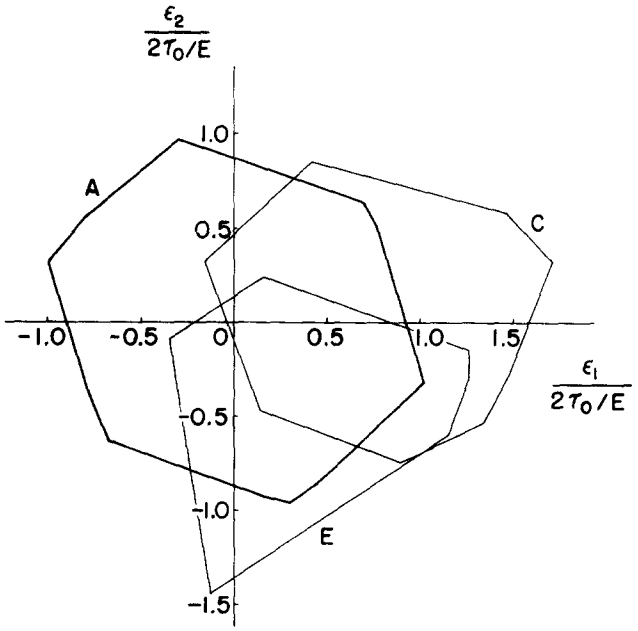

FIG. 13. Superposition of initial yield surface (A) in strain space with subsequent yield surfaces at C and E.

vertices displayed in Figs. 6–8. Nevertheless, we see the characteristic tendencies of macroscopic yield surfaces in these figures (e.g. translation, shape change, etc.). Moreover, if we were to calculate a yield surface based upon a very small but finite amount of additional plastic strain as criterion (which has been done by Lin and Ito [28] for their model), it is expected that this surface, too, would exhibit a smooth but sharply rounded curve lying within the fan of critical systems at the stress point. Finally, it is the predicted stress–strain curves (rather than yield surfaces) to which one probably should direct the most attention since their experimental counterparts are less sensitive to differing definitions and measurement techniques. In a future study we intend to pursue a comparison for the case of (nearly) uniaxial stressing well into the plastic range. (In the present study, with its emphasis on a partial loading-reverse loading cycle and abrupt changes in strain path, the largest macroscopic plastic strain increments computed were only two to three times the corresponding elastic increments.)

Acknowledgements—The work of one of us (R.V.) was supported entirely by the Office of Naval Research, Contract No. N00014-68-A-0187, through a graduate research assistantship. The preparation of this paper was supported in part by the National Science Foundation under Grant GK-31313.

REFERENCES

[1] K. S. HAVNER, A discrete model for the prediction of subsequent yield surfaces in polycrystalline plasticity. *Int. J. Solids Struct.* 7, 719 (1971).

[2] K. S. HAVNER, On convergence of a discrete aggregate model in polycrystalline plasticity. *Int. J. Solids Struct.* 7, 1269 (1971).

[3] K. S. HAVNER, An analytical model of large deformation effects in crystalline aggregates, *Symposium on Foundations of Plasticity*, edited by A. SAWCZUK, Noordhoff, in press.

[4] R. HILL, Generalized constitutive relations for incremental deformation of metal crystals by multislip. *J. Mech. Phys. Solids* **14**, 95 (1966).
[5] R. HILL, The essential structure of constitutive laws for metal composites and polycrystals. *J. Mech. Phys. Solids* **15**, 79 (1967).
[6] R. HILL, The mechanics of quasi-static plastic deformation in metals, *Surveys in Mechanics* (G. I. Taylor 70th Anniversary Volume), pp. 7–31. Cambridge University Press (1956).
[7] J. MANDEL, Generalisation de la theorie de plasticite de W. T. Koiter. *Int. J. Solids Struct.* **1**, 273 (1965).
[8] W. M. MAIR and H. LL. D. PUGH, Effect of pre-strain on yield surfaces in copper. *J. mech. Engng Sci.* **6**, 150 (1964).
[9] M. RONAY, Second-order elongation of metal tubes in cyclic torsion. *Int. J. Solids Struct.* **4**, 509 (1968).
[10] J. F. W. BISHOP and R. HILL, A theory of the plastic distortion of a polycrystalline aggregate under combined stresses. *Phil. Mag., ser.* 7, **42**, 414 (1951).
[11] U. F. KOCKS, Polyslip in polycrystals. *Acta Met.* **6**, 85 (1958).
[12] R. HILL, Elastic properties of reinforced solids: some theoretical principles. *J. Mech. Phys. Solids* **11**, 357 (1963).
[13] R. HILL, On constitutive macro-variables for heterogeneous solids at finite strain. *Proc. R. Soc., Lond.* **A326**, 131 (1972).
[14] W. PRAGER, Recent developments in the mathematical theory of plasticity. *J. appl. Phys.* **20**, 235 (1949).
[15] D. C. DRUCKER, Some implications of work hardening and ideal plasticity. *Q. appl. Math.* **7**, 411 (1950).
[16] D. C. DRUCKER, A more fundamental approach to plastic stress–strain relations. *Proc 1st U.S. natn. Congr. appl. Mech.*, pp. 487–491 (1951).
[17] D. TRIFAN, Stress theory of plastic flow. *J. Math. Phys.* **35**, 44 (1956).
[18] T. H. LIN, Physical theory of plasticity, *Advances in Applied Mechanics* **11**, 255–311. Academic Press (1971).
[19] J. R. RICE, On the structure of stress–strain relations for time-dependent plastic deformation in metals. *J. appl. Mech.* **37**, 728 (1970).
[20] G. I. TAYLOR, The distortion of aluminum crystals under compression, Part II. *Proc. R. Soc., Lond.* **A116**, 16 (1927).
[21] G. I. TAYLOR, Plastic strain in metals. *J. Inst. Metals* **62**, 307 (1938).
[22] R. VARADARAJAN, A Quantitative Study of a Mathematical Model for Plastic Deformation of Crystalline Aggregates, Ph.D. Thesis, North Carolina State University (1972).
[23] H. P. KÜNZI and W. KRELLE, *Nonlinear Programming*, Chap. 5. Blaisdell (1966).
[24] U. F. KOCKS, The relation between polycrystal deformation and single-crystal deformation. *Metall. Trans.* **1**, 1121 (1970).
[25] M. A. JAWSON and M. H. RICHMAN, A critical review of the effects of grain boundaries on the mechanical properties of materials. *Appl. Mech. Rev.* **17**, 857 (1964).
[26] J. W. HUTCHINSON, Elastic–plastic behavior of polycrystalline metals and composites. *Proc. R. Soc., Lond.* **A319**, 247 (1970).
[27] A. PHILLIPS and J. L. TANG, The effect of loading path on the yield surface at elevated temperatures. *Int. J. Solids Struct.* **8**, 463 (1972).
[28] T. H. LIN and M. ITO, Theoretical plastic stress-strain relationship of a polycrystal and the comparisons with the von Mises and the Tresca plasticity theories. *Int. J. Engng Sci.* **4**, 543 (1966).
[29] J. F. NYE, *Physical Properties of Crystals*, Chap. 8. Oxford University Press (1957).

APPENDIX

The kth row vector of the transformation matrix $\mathbf{N}$ is given in terms of unit vectors $\mathbf{n}^k$, $\mathbf{b}^k$ in the normal and glide directions, respectively, of the kth crystallographic slip system as

$$\mathbf{N}_k = \left[n_1^k b_1^k, n_2^k b_2^k, n_3^k b_3^k, \frac{1}{\sqrt{2}}(n_2^k b_3^k + n_3^k b_2^k), \frac{1}{\sqrt{2}}(n_3^k b_1^k + n_1^k b_3^k), \frac{1}{\sqrt{2}}(n_1^k b_2^k + n_2^k b_1^k) \right]. \quad \text{(A1)}$$

In terms of $\mathbf{N}_c$ (corresponding to the lattice axes), $\mathbf{N} = \mathbf{N}_c\mathbf{A}$, with $\mathbf{n}_c^k$, $\mathbf{b}_c^k$ defined by the family of crystallographically equivalent slip systems $\{111\}\langle 1\bar{1}0\rangle$. The six by six transformation matrix $\mathbf{A}$ is determined from the orthogonal lattice orientation matrix $R_{Ji} = \cos(\xi_J, x_i)$.

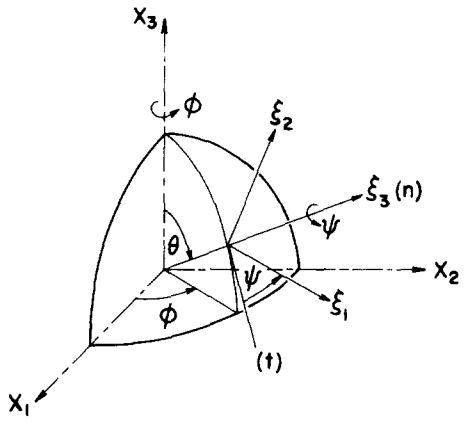

FIG. A1. Euler angles of crystal lattice axes.

From Fig. A1, **R** is given by

$$\mathbf{R} = \begin{bmatrix} \cos\psi\cos\theta\cos\phi - \sin\psi\sin\phi & \cos\psi\cos\theta\sin\phi + \sin\psi\cos\phi & -\cos\psi\sin\theta \\ -\sin\psi\cos\theta\cos\phi - \cos\psi\sin\phi & -\sin\psi\cos\theta\sin\phi + \cos\psi\cos\phi & \sin\psi\sin\theta \\ \sin\theta\cos\phi & \sin\theta\sin\phi & \cos\theta \end{bmatrix}. \tag{A2}$$

The symmetric, crystal elastic compliance $\mathbf{C}_c$ for aluminum, in units of 10^{-3} mm^2/kg (as converted from [29]), has elements $(C_c)_{11} = (C_c)_{22} = (C_c)_{33} = 0{\cdot}1559$, $(C_c)_{12} = (C_c)_{13} = (C_c)_{23} = -0{\cdot}0569$, $(C_c)_{44} = (C_c)_{55} = (C_c)_{66} = 0{\cdot}1726$, with all other non-symmetric elements zero, and we have $\mathbf{C} = \mathbf{A}^T\mathbf{C}_c\mathbf{A}$.

Lastly, the operator $\mathscr{D}$ is given by

$$\mathscr{D} = \begin{bmatrix} \partial_1, & 0, & 0, & 0, & \frac{1}{\sqrt{2}}\partial_3, & \frac{1}{\sqrt{2}}\partial_2 \\ 0, & \partial_2, & 0, & \frac{1}{\sqrt{2}}\partial_3, & 0, & \frac{1}{\sqrt{2}}\partial_1 \\ 0, & 0, & \partial_3, & \frac{1}{\sqrt{2}}\partial_2, & \frac{1}{\sqrt{2}}\partial_1, & 0 \end{bmatrix} \tag{A3}$$

wherein ∂_i denotes partial differentiation with respect to the corresponding spatial coordinate.

(*Received* 19 *June* 1972)

Абстракт—С целью исследования теоретического макроскопического поведения гранецентраированных кубических металлических поликристаллов применяется дискретная совокупная модель, Вобще, проверяются дуальные неравенства макроскопической теории пластичности и показываются, на последующих поверхностях течения, как для пространства напряжений так и деформаций, в качестве рассчитанных для алюминия под влиянием двухосной деформации. Указано, что предсказанные кривые напряжения-деформация соответствуют частному циклу нагрузки и разгрузки. Совокупная модель содержит в себе несколько тысяч кристаллографических систем скольжения. Получаются все количественные результаты вследствие решения задач стесненного квадратического программирования, определяющих постепенно нарастающие сдвиги кристаллов.